Human Molecular Genetics, 2007, Vol. 16, No. 6 **651–666**
doi:10.1093/hmg/ddm008
Advance Access published on February 19, 2007

Over-expression of alpha-synuclein in human neural progenitors leads to specific changes in fate and differentiation

Bernard L. Schneider[1,2], Corey R. Seehus[1], Elizabeth E. Capowski[1], Patrick Aebischer[2], Su-Chun Zhang[1] and Clive N. Svendsen[1,*]

[1]Waisman Center and Department of Anatomy, University of Wisconsin, 1500 Highland Avenue, Madison, WI 53705, USA and [2]Brain & Mind Institute, Ecole Polytechnique Fédérale de Lausanne (EPFL), Switzerland

Received December 04, 2006; Revised January 29, 2007; Accepted January 30, 2007

Missense mutations and extra copies of the α-*Synuclein* gene result in Parkinson disease (PD). Human stem and progenitor cells can be expanded from embryonic tissues and provide a source of non-transformed neural cells to explore the effects of these pathogenic mutations specifically in human nervous tissue. We over-expressed the wild type, A53T and A30P forms of α-synuclein in expanded populations of progenitors derived from the human fetal cortex. The protein localized in the nucleus and around micro-vesicles. Only the A53T form was acutely toxic, suggesting a unique vulnerability of these progenitors to this mutation. Interestingly, constitutive over-expression of wild-type α-synuclein progressively impaired the innate ability of progenitors to switch toward gliogenesis at later passages. To explore the effect of α-synuclein on neuronal subtypes selectively affected in PD, such as dopaminergic neurons, α-synuclein and its mutations were also over-expressed in terminally differentiating neuroectodermal cultures derived from human embryonic stem cells (hESC). Alpha-synuclein induced acute cytotoxicity and reduced the number of neurons expressing either tyrosine hydroxylase or gamma-aminobutyric acid over time. Consistent with the selective vulnerability of ventral midbrain dopaminergic neurons, α-synuclein cytotoxicity appeared most pronounced following FGF8/SHH specification and was decreased by inhibition of dopamine synthesis. Together, these data show that α-synuclein over-expressed in human neural embryonic cells results in patterns of degeneration that in some cases match features of Parkinson Disease. Thus, neural cells derived from hESC provide a useful model system to understand the development of α-synuclein-related pathologies and allow therapeutic drug screening.

INTRODUCTION

Missense mutations (A53T, A30P and E46K) (1–3), duplication (4) and triplication (5) of the α-*Synuclein* gene (PARK1 locus) have been found to cause autosomal dominant Parkinson disease (PD). Thus, both increased α-*Synuclein* gene dosage and mutations favoring its conversion to abnormally folded species forming oligomers appear to cause PD. Alpha-synuclein oligomers ultimately develop into fibrils, the main constituent of Lewy bodies (6). These protein aggregates are considered a hallmark of synucleinopathies, a class of disorders that affects various brain regions, including the cerebral cortex and the *substantia nigra pars compacta*.

Alpha-synuclein is expressed in neural cell soma during development from week 11, but the protein is then redistributed to the nerve terminals within the adult brain (7–9). Although a role for α-synuclein has been proposed in synaptic transmission (10), its function remains unclear and might vary with its intracellular localization and the stage of neuronal maturation.

Over-expression of both wild type and mutated forms of α-synuclein has been used to develop genetic models of the disease in yeast (11), *Caenorhabditis elegans* (12), *Drosophila* (13), mice (14–16), rats (17,18) and primates (19). While of great interest, these models often fail to reproduce cardinal features of the disease. For example, the loss of nigral dopa-

*correspondence should be addressed. Tel: +1 6082658668; Fax: +1 6082635267; Email: svendsen@waisman.wisc.edu

minergic neurons is rarely observed in α-synuclein transgenic mice (14,15). Although α-synuclein over-expression in invertebrates leads to remarkable phenotypes, the absence of any endogenous α-synuclein homolog constitutes a caveat in these models. Clearly, there is a need to complement animal models with *in vitro* human systems to elucidate the specificities of the human condition (20).

Recently, culture systems have been defined to expand stem and progenitor cells from human embryonic tissues. These cells provide both a unique window on human development and a renewable source of non-transformed neural cells. Human neural progenitors derived from the fetal cortex (hNPC^{ctx}) mostly differentiate into small bipolar interneurons and follow a time-dependent transition from neuronal to glial fate that mimics human cortical development during their 30–50 week expansion *in vitro* (21,22). Human embryonic stem cells (hESC) derived from the inner cell mass of the blastocyst (23), can be efficiently differentiated into neuroepithelial cells that produce subsets of long-projection neurons, such as motoneurons (24) and dopaminergic neurons (25,26) upon exposure to specific morphogens. These neurons formed *in vitro* present morphological, biochemical and physiological properties similar to their *in vivo* counterparts, although their functional properties remain to be tested.

Both of these cell sources offer great promise to develop human genetic models of neurodegeneration. In the present study, we have developed a system of lentiviral infection to determine the effects of α-synuclein over-expression on the fate and survival of both neural progenitors and differentiating neuronal populations.

RESULTS

Human NPC^{ctx} express truncated and oligomeric forms of α-synuclein

We first confirmed that α-synuclein mRNA was present in wild-type hNPC^{ctx} by real-time PCR (data not shown) and determined what form of α-synuclein was present in native hNPC^{ctx} and how this compared to those over-expressing α-synuclein. In protein extracts of cells over-expressing α-synuclein, the LB509 antibody (epitope: amino acids 115–122) recognized a 16 kD band corresponding to the full length protein but failed to recognize any protein in native hNPC^{ctx} (Fig. 1). As C-terminal α-synuclein truncations have been described in human cell and brain extracts (27), we used two antibodies recognizing a more N-terminal portion of the protein: the polyclonal antibody AB5038 (epitope: amino acids 111–131) and the monoclonal antibody Syn204 (epitope: amino acids 102–110). While these two antibodies recognized the over-expressed full-length form, they also detected a shorter form of α-synuclein, present in both native hNPC^{ctx} and over-expressers (Fig. 1). To detect full-length forms of α-synuclein, we enriched cytosolic protein extracts of hNPC^{ctx} by immunoprecipitation using the monoclonal antibody Syn211 (epitope: amino acids 120–125) and used the LB509 antibody for immunodetection. In addition to the over-expressed full-length monomer in αSyn WT hNPC^{ctx}, high molecular weight species migrating as a 36 kD doublet (**) and 30 kD band (*) could be detected in protein extracts of both native and infected cortical progenitors (Supplementary Material, Fig. S1A). In the absence of immunoprecipitation, the LB509 antibody weakly recognized a similar 36 kD doublet in nuclear protein extracts of non-infected hNPC^{ctx} (Supplementary Material, Fig. S1B). These bands might correspond to either ubiquitinated or oligomeric forms of α-synuclein (28).

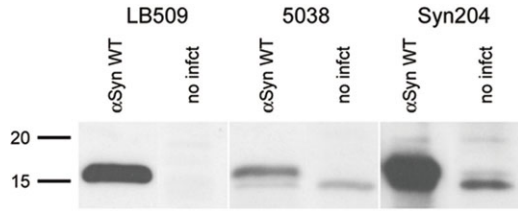

Figure 1. Alpha-synuclein expression in hNPC^{ctx}. Western blot analysis of α-synuclein expression in hNPC^{ctx} either uninfected or infected with a lentivirus for αSynWT over-expression. Three antibodies were used: LB509, AB5038 and Syn204.

Together, these results show that α-synuclein is expressed at low levels in cultured native progenitors of the human cortex. The protein seems to undergo extensive post-translational modifications, such as truncation and oligomerization. When over-expressed using lentiviral vectors, the 16 kD full-length form accumulates in hNPC^{ctx}.

Establishment of transgenic hNPC^{ctx} populations over-expressing α-synuclein and its mutants: mutation-dependent expression levels

We next sought to establish transgenic populations of hNPC^{ctx} to determine the effect of α-synuclein over-expression on hNPC^{ctx} phenotype. Human neural progenitors were derived from the fetal cortex (age 87–94 days, donors M006, M031, M045 and M046) and grown as neurospheres for more than 30 weeks *in vitro*. During that time, they progressively switch from an essentially neurogenic fate to a mainly gliogenic fate. At 10–20 weeks of expansion, transiently dissociated neurospheres were infected by exposure to lentiviral vectors coding for α-synuclein WT (αSyn WT), A30P or A53T (Fig. 2A). The progenitors then reformed spheres that could be expanded in the presence of EGF/LIF and compared with either non-infected or GFP-infected hNPC^{ctx}.

Four days following infection, we could detect over-expression of GFP (Fig. 2B) and α-synuclein (Fig. 2C, immunocytochemistry with the LB509 antibody) in hNPC^{ctx}. The wild type and A53T forms displayed both a nuclear and a punctate cytoplasmic staining while the A30P form appeared more homogenously distributed. At this early stage, transgene over-expression could be detected in $>75\%$ of the cells in every condition. After 1 month of expansion, the number of integrated transgene genomic copies was assessed in hNPC^{ctx} derived from three independent donors (M031, M045 and M046). Five infections of hNPC^{ctx} populations led to similar relative numbers of transgene copies for each lentivirus based on qPCR (Fig. 2D), within a range of 5–10 integrated copies/cell. This confirmed the comparable efficiency of each of the four lentivirus preparations.

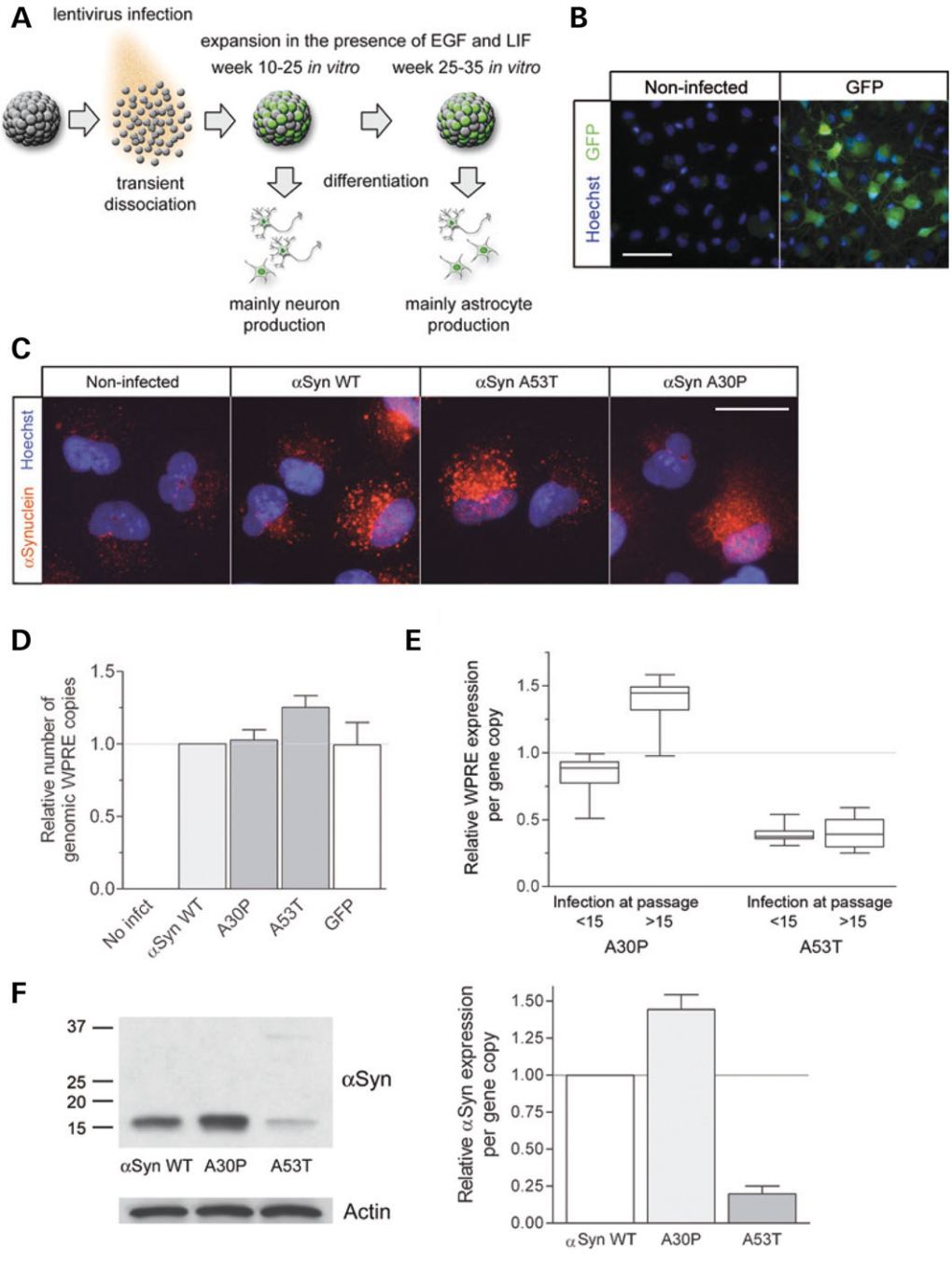

Figure 2. Quantification of transgene integration and expression following lentivirus infection. (**A**) Schema of the hNPC^{ctx} culture system: transgenic populations were obtained by lentiviral infection of dissociated neurospheres. Over time in culture, the fate of hNPC^{ctx} evolves from neuronal toward glial cell production. (**B**) GFP expression in transgenic and non-infected populations of hNPC^{ctx}. Scale bar 40 μm. (**C**) Immunocytochemistry of α-synuclein expression in hNPC^{ctx} (LB509). Note the low level of expression in the non-infected cells and the diffuse distribution of the A30P mutant. Scale bar 10 μm. (**D**) Relative quantification of integrated transgene copy numbers (WPRE normalized with respect to albumin) in five transgenic populations of hNPC^{ctx} (**E**) Box-and-Whisker plot showing the transgene expression levels of α-synuclein mutants per transgene copy (WPRE expression normalized with respect to β-actin). Mutants are compared with αSynWT (arbitrarily set at 1) in four populations of hNPC^{ctx}, infected either before passage 15 or after passage 15. Note the relatively low level of expression of the A53T form and the increase in A30P expression as a function of the time of infection. (**F**) Representative western blot and quantification of protein expression per gene copy in three populations of hNPC^{ctx} over-expressing α-synuclein and its mutants (LB509 antibody, α-synuclein normalized with respect to α-actin).

Relative amounts of WPRE mRNA expressed per gene copy were then determined for each infected population of hNPC^{ctx}. When compared with αSyn WT, divergent levels of expression were obtained for the two mutants (Fig. 2E). In four independent infections (M031 and M046 donors) performed before passage 15, A53T expression was significantly decreased when compared with the two other forms (−60%). In four infections performed after passage 15 in culture, we

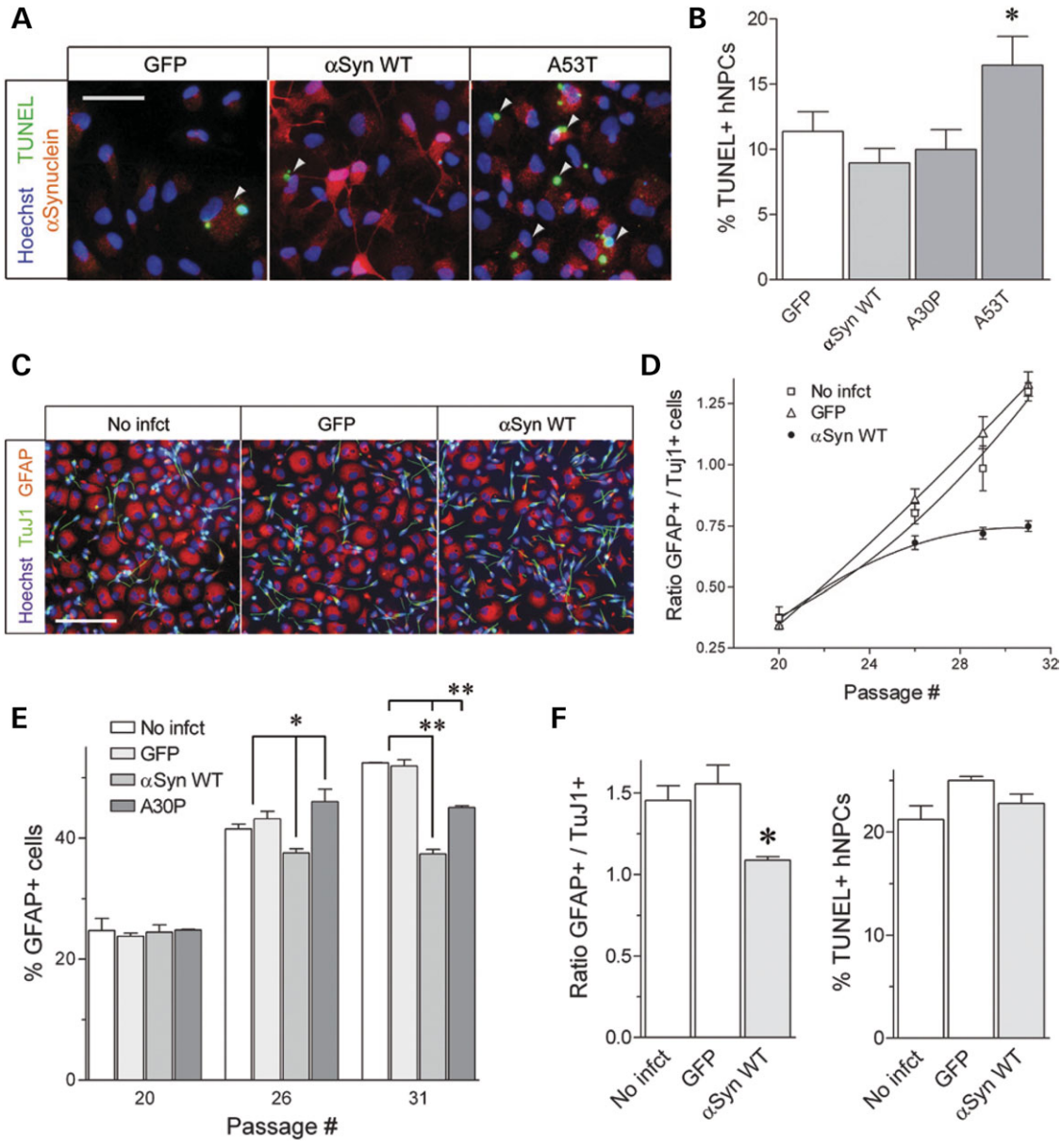

Figure 3. Analysis of progenitor fate and survival in response to α-synuclein over-expression. (**A**) TUNEL staining and α-synuclein immunocytochemistry on hNPC^{ctx} 4 days after lentiviral infection. Arrowheads indicate TUNEL+ cells. Scale bar 40 μm. (B) Quantification of TUNEL+ cells in four populations of hNPC^{ctx} derived from four independent donors, 4 days post-infection ($^{*}P < 0.01$ versus GFP, $P < 0.001$ versus αSynWT and A30P). (**C**) Immunocytochemistry for GFAP (red) and TuJ1 (green) on hNPC^{ctx} (passage 31) differentiated for 7 days. Scale bar 100 μm (**D**) Quantification of M031 neurosphere differentiation over time in culture, expressed as the ratio of GFAP+ cells with an astrocytic morphology over TuJ1+ neuronal cells. Progenitors over-expressing αSyn WT are compared with control cultures (non-infected and GFP-infected). Data are expressed as mean ± SD, $n = 3$ for each condition. (**E**) Percentage of GFAP+ produced after 7 days of differentiation at passage 20, 26 and 31 in the M031 hNPC^{ctx}. $^{*}P < 0.05$, $^{**}P < 0.001$; n=3 for each condition. (**F**) Differentiation (7 days) and survival, expressed as a percentage of TUNEL+ cells, in dissociated cultures of M031 hNPC^{ctx} at passage 29. $^{*}P < 0.05$, $n = 3$.

noticed a higher expression level of the A30P mutant when compared with αSyn WT (M031, M045 and M046 donors, +36%). The A53T form was again expressed at relatively low levels (−59%).

To confirm a similar effect on protein expression, we assessed α-synuclein levels by western blotting (LB509 antibody, Fig. 2F). Endogenous 16 kD α-synuclein is not detected in these conditions (see Fig. 1). In over-expressers, the LB509 antibody recognizes specifically a 16 kD band, with a 35 kD oligomeric form detectable in cells over-expressing the A53T mutant. Semi-quantitative determination of α-synuclein expression per transgene copy in hNPC^{ctx} infected after passage 15 (M031, M045 and M046 donors), revealed the same divergence in protein expression levels: 44% increase of the A30P form and an 80% decrease for the A53T form, when compared with αSyn WT.

These data show that hNPC^{ctx} tightly regulate their level of α-synuclein over-expression following lentiviral transduction, as a function of both time of infection and pathogenic mutation. This observation suggests adaptive effects in the

hNPC^{ctx} populations that, in the case of the A53T mutation, eliminate cells with high transgene expression levels. This result prompted us to assess carefully how hNPC^{ctx} respond to α-synuclein over time in culture.

Over-expression of the A53T α-synuclein mutant induces acute cell death in hNPC^{ctx}

The lower level of α-synuclein expression in the A53T hNPC^{ctx} might indicate a cytotoxic effect leading to the loss of high expressers. To determine if that was indeed the case, hNPC^{ctx} derived from the M006, M031, M045 and M046 donors were infected in parallel with the GFP, αSyn WT, A30P and A53T lentiviruses. Four days after infection, α-synuclein cytotoxicity was analyzed by TUNEL (Fig. 3A and B). Percentage of TUNEL+ cells following αSyn WT and A30P infections was 9.0 ± 1.1 and 10.0 ± 1.5, respectively, a value similar to the GFP infection ($11.4 \pm 1.5\%$). An identical titer of the A53T lentivirus induced significantly higher cell death, with $16.4 \pm 2.2\%$ of TUNEL+ cells averaged over the four independent populations of hNPC^{ctx} ($P < 0.01$ versus GFP, $P < 0.001$ versus αSyn WT and A30P, repeated measures ANOVA).

Thus, over-expression of the A53T mutant induces acute toxic effects in hNPC^{ctx} that prevent the establishment of expression levels comparable to the two other α-synuclein forms. For this reason, further analysis of the α-synuclein effects in hNPC^{ctx} lines was focused on the αSyn WT and A30P variants.

Induced over-expression of αSyn WT prevents the progressive switch of hNPC^{ctx} to glial cell production

We next explored whether α-synuclein over-expression in hNPC^{ctx} affected their ability to differentiate into neurons (TuJ1+) and astrocytes (GFAP+, astrocytic morphology). Expanded neurospheres were induced to differentiate for 7 days and their progeny analyzed for TuJ1 and GFAP (donor M031, Fig. 3C and D). At 7 weeks post-infection (passage 20), hNPC^{ctx} generated ∼67% TuJ1+ neurons and 24% GFAP+ astrocytes (ratio GFAP+/TuJ1+ = 0.35–0.37) in non-infected, GFP and αSyn WT populations. As expected, the proportion of neurons produced upon differentiation decreased progressively over time, in both uninfected and GFP hNPC^{ctx}, leading to the production of a majority of GFAP+ cells with an astrocytic morphology at passage 31 (ratio of GFAP+/TuJ1+ = 1.30–1.33) (Fig. 3D and E). Interestingly, hNPC^{ctx} over-expressing αSyn WT showed a significant reduction in the number of astrocytes versus neurons produced at passage 26 and 31 (Fig. 3D and E). At passage 31, the ratio GFAP+/TuJ1+ was only 0.75 ± 0.02 (SD) in the differentiated αSyn WT hNPC^{ctx}; $P < 0.001$ when compared with controls. A similar lack of gliogenesis was observed in hNPC^{ctx} derived from the M046 donor (data not shown).

A30P α-synuclein also impaired the production of GFAP+ glial cells in M031 hNPC^{ctx} at passage 31, when compared with the non-infected and GFP progenitors (Fig. 3E). Nevertheless, A30P hNPC^{ctx} consistently produced more GFAP+ cells than the αSyn WT over-expressers, both at passages 26 and 31 ($P < 0.001$). This suggests a pro-gliogenic effect of the A30P mutation when compared with αSyn WT. Again, hNPC^{ctx} derived from the M046 donor showed a similar pattern (data not shown).

To analyze whether α-synuclein induced selective cell death during differentiation, M031 hNPC^{ctx} were dissociated at passage 29 and induced to differentiate for 7 days. We then determined both the ratio of GFAP+/TuJ1+ cells and percentage of TUNEL+ cells. As expected, αSyn WT over-expression led to a significant reduction in the ratio GFAP+/TuJ1+ (1.08 ± 0.02 for αSyn WT versus 1.45 ± 0.09 and 1.56 ± 0.11 for the non-infected and GFP controls, standard error of the mean (SEM), $P < 0.05$) (Fig. 3F). We did not observe any significant difference in the percentage of TUNEL+ cells, showing that the effect of α-synuclein on the fate of cortical progenitors was not mediated by selective cell death in their progeny. Together, these data suggest that α-synuclein over-expression prevents the progressive switch of hNPC^{ctx} toward glial cell production, an effect that does not depend on cell death.

When over-expressed, α-synuclein affects the proliferation of gliogenic precursors and localizes both in the cell nucleus and around cytoplasmic microvesicles

We next sought to determine whether α-synuclein might affect the proliferation of hNPC^{ctx}, preventing the establishment of normal astrogliogenesis. As the mixed fate of hNPC^{ctx} can confound the analysis of progenitor proliferation, we modified the culture conditions to establish a population of progenitors with mostly a glial fate. Neurosphere cultures were first grown for 28–30 passages in response to EGF alone until they stopped proliferating. At that time, LIF was added in the culture medium, stimulating for 6 additional weeks the growth of hNPC^{ctx} with a mostly glial fate (>75% GFAP+ cells after 7 days of differentiation).

In these conditions, we measured the proliferation rate of hNPC^{ctx} derived from the M046 donor at passage 31 by determining nuclear Ki67 immunoreactivity (Fig. 4A and B). We observed a significant decrease in the percentage of Ki67+ nuclei in response to αSyn WT ($17.1 \pm 0.8\%$ versus $23.4 \pm 1.7\%$ (non-infected) and $21.7 \pm 1.3\%$ (GFP), SEM, $P < 0.05$). Progenitors expressing the A30P mutant had a proliferation rate significantly higher than the αSyn WT over-expressers, with $21.0 \pm 1.2\%$ of Ki67 + nuclei ($P < 0.05$). A similar effect was observed in the M031 line, when cell proliferation was measured by bromodeoxyuridine (BrdU) pulsing (Supplementary Material, Fig. S2).

Thus, αSyn WT over-expression decreases the proliferation rate of gliogenic progenitors. When compared with αSyn WT, the A30P mutation facilitates glial progenitor proliferation. This difference in the cell response to these two α-synuclein forms parallels the observed differences in the relative transgene expression levels (Fig. 2D), with a higher level of A30P protein in progenitors infected at later, more gliogenic passages.

In the same culture conditions, immunocytochemistry using the LB509 antibody revealed a punctate staining of αSyn WT in the cytoplasm, and a diffuse nuclear distribution (Fig. 4C). Cells over-expressing A30P showed a more diffuse localiz-

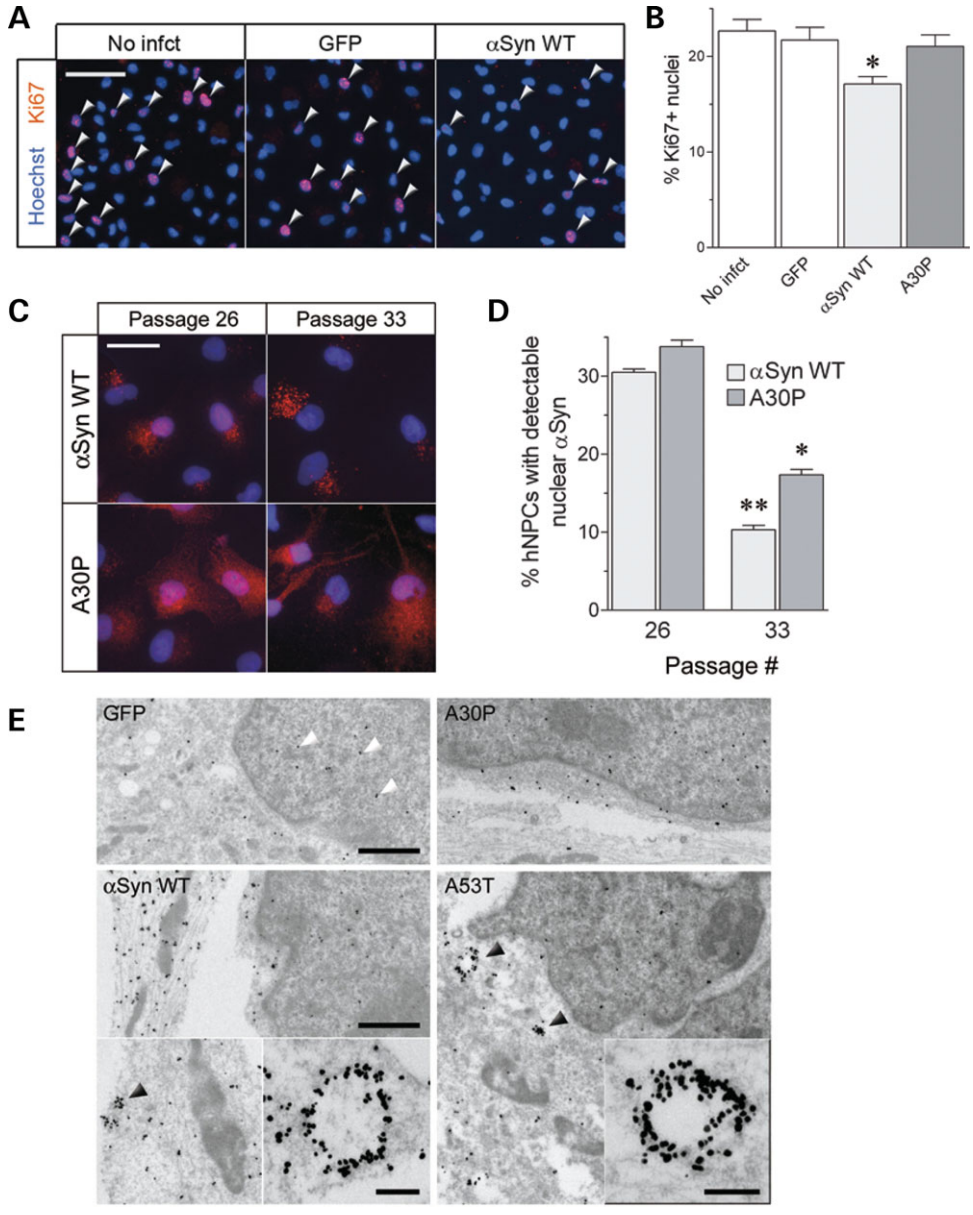

Figure 4. Progenitor proliferation and α-synuclein subcellular localization (**A**) Ki67 immunocytochemistry on M046 hNPC^{ctx}. Arrowheads indicate Ki67 + nuclei. Scale bar 50 μm (**B**) Proliferation of gliogenic hNPC^{ctx} (M046 donor, passage 31), as determined by the percentage of Ki67+ nuclei. $^{*}P < 0.05$, $n = 3$ for each condition. (**C**) Alpha-synuclein immunocytochemistry in M031 hNPC^{ctx} over-expressing αSyn WT and A30P. Note the decrease in αSyn WT nuclear localization between passage 26 and 33 (mainly gliogenic progenitors) in culture. (**D**) Quantification shows a significantly higher nuclear localization of over-expressed α-synuclein carrying the A30P mutation at passage 33. Scale bar 25 μm, $^{**}P < 0.01$ versus A30P, $P < 0.001$ versus passage 26, $^{*}P < 0.001$ versus passage 26; $n = 3$ for each condition, two-way ANOVA. (**E**) Immunogold labeling of α-synuclein and electron microscopy on M046 hNPC^{ctx}. Note α-synuclein presence in the cell nucleus (white arrowheads) and clustering around microvesicles (black arrowheads). In cells over-expressing the A30P mutant, α-synuclein clusters are rarely observed. Scale bars: 2 μm and 0.5 μm (insets showing microvesicles).

ation throughout the cell, including the nucleus. We next compared the distribution of over-expressed αSyn WT and A30P in hNPC^{ctx} populations with a predominantly neuronal fate (passage <26, ratio GFAP+/TuJ1+ cells ≤1) or mainly glial fate (passage >30, ratio GFAP+/TuJ1+ cells >3) (M031, Fig. 4D). At early passages, both wild-type and A30P α-synucleins were clearly present in the nuclei in ∼30% of hNPC^{ctx}. The nuclear staining appeared diffuse and was easily distinguishable from the punctate cytoplasmic staining. In cells with mostly a glial fate (passage 33), αSyn WT appeared mainly clustered in the cytoplasm ($10.3 \pm 0.6\%$ nuclear localization, $P < 0.001$ when compared to passage 26). With the A30P mutant, a larger proportion of progenitors displayed nuclear localization ($17.3 \pm 0.7\%$, $P < 0.01$ when compared to αSyn WT). These data were confirmed in hNPC^{ctx} derived from the M046 donor (data not shown). Thus, there is a shift in the sub-cellular localization of α-synuclein over time in culture, correlating with the

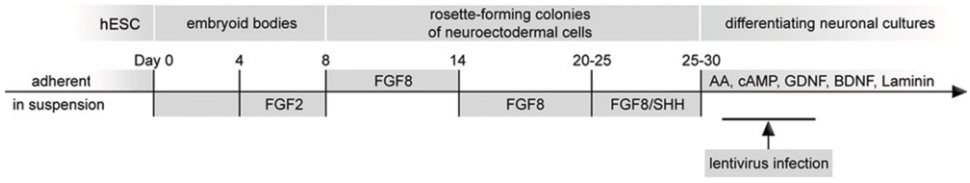

Figure 5. Schema of the hESC differentiation protocol. Human ESC are differentiated following a stepwise protocol in chemically defined conditions. Initial differentiation is induced by the formation of embryoid bodies, followed by neural induction in the presence of FGF2. For neural specification, adherent colonies are exposed to FGF8 for rostro-caudal specification. Neurosphere cultures are further patterned with SHH (dorso-ventral specification). Dissociated cultures of neuroepithelial are exposed to lentiviral vectors for α-synuclein over-expression during the terminal step of differentiation.

change in the fate of the progenitors. This re-distribution is disrupted by the A30P mutation.

Control lines and α-synuclein over-expressers derived from the M046 donor and grown continuously in EGF and LIF were immunogold-labelled for α-synuclein (AB5038 antibody) and analyzed by transmission electron microscopy (TEM) (Fig. 4E). Alpha-synuclein was detected both in the cytoplasm and nucleus of all lines, and when over-expressed, frequently formed clusters around cytoplasmic microvesicles of unknown function. In contrast to wild-type and A53T α-synuclein, the A30P mutant protein was rarely observed in clusters, consistent with its reduced affinity for membranes (11,29,30).

Human ES cells: a source of long projection neurons that can be genetically modified to over-express α-synuclein

We next wanted to establish the effects of α-synuclein in human dopaminergic neurons derived from stem cells. Due to regional specification at the time of tissue collection, expanded progenitors derived from the developing human brain produce only a limited set of neuronal cell types that do not include dopaminergic neurons, even when generated from the mesencephalon (31,32). To address this issue, we used hESC as a source of neuroectoderm producing long projection neurons, including dopaminergic neurons (Fig. 5). Colonies of hESC (H9 line) were differentiated into adherent neuroepithelial cells in the presence of FGF2. As described previously, sequential exposure to FGF8 and sonic hedgehog (SHH) specifies a progenitor population that further matures into neurons with a set of markers and physiological properties similar to the ventral midbrain dopaminergic neurons (25,26).

Neuroepithelial cells were positive for nestin, a marker of neural progenitor cells, and continuously produced cells expressing neuronal markers such as TuJ1 and Map2ab (Fig. 6A). Using the GFP lentiviral vector, we obtained high transduction efficiency of differentiating neuroepithelial progenitors and neurons. GFP expression, detected from day 4 after infection, was still present in >70% of the cells 22 days post-infection and maintained in neuronal cells expressing tyrosine hydroxylase (TH) (Fig. 6B). Using the previously characterized lentiviral vectors coding for αSyn WT, A30P and A53T, we could detect transgene over-expression 22 days post-infection (Fig. 6C). It was of interest that non-infected cells with a neuronal morphology showed a faint α-synuclein staining in their cytoplasm, suggesting a low level of endogenous expression.

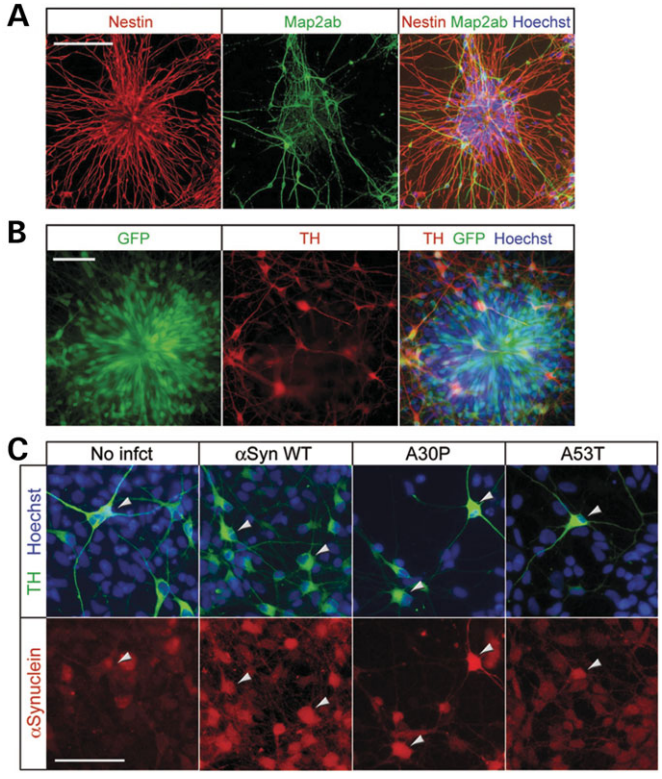

Figure 6. Terminal differentiation of neuroepithelial cells. (**A**) Nestin (red) and Map2ab (green) immunocytochemistry on neuroepithelial cells derived from the H9 hESC line on day 10 of terminal differentiation. Scale bar 100 μm. (**B**) GFP expression in differentiating cultures of neuroepithelial cells (day 22 of terminal differentiation, 21 days post-infection). Immunocytochemistry for TH (red) demonstrates the presence of dopaminergic neurons over-expressing GFP. Scale bar 50 μm. (**C**) Alpha-synuclein expression (LB509 antibody, red) in differentiating neuronal cultures derived from hESC. Arrowheads indicate TH+ cells (green) staining positively for α-synuclein. Note the presence of a low level of endogenous α-synuclein (non-infected neurons) and the detectable over-expression at day 22 of terminal differentiation (21 days post-infection). Scale bar 50 μm.

Over-expression of α-synuclein is cytotoxic to differentiating cultures of neuroepithelial cells specified with FGF8 and SHH

Neuroepithelial cells obtained as described in Fig. 5 were specified with FGF8 and SHH. After 3 days of terminal differentiation, cells were infected with lentiviral vectors (4 ng p24) coding either for GFP, αSyn WT, A30P or A53T. Four days

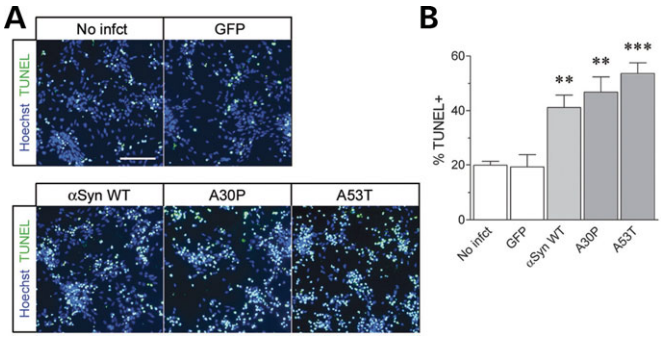

Figure 7. Cytotoxicity of α-synuclein over-expression in terminally differentiating neuronal cultures derived from hESC. (**A**) TUNEL staining at day 7 of differentiation, 4 days post-infection. Scale bar 100 μm. (**B**) Quantification of TUNEL+ cells. $^{**}P < 0.01$, $^{***}P < 0.001$, $n = 4$ for each condition.

post-infection, we analyzed cell death by TUNEL staining (Fig. 7A). Infection with the GFP vector had no detectable toxicity in these conditions, with 19.2 ± 4.6% TUNEL+ nuclei versus 19.9 ± 1.5% in the absence of infection (Fig. 7B). All three α-synuclein forms induced cell death, with 41.2 ± 4.5% (αSyn WT), 46.8 ± 5.6% (A30P) and 53.6 ± 3.9% (A53T) of TUNEL+ nuclei detected for each condition (Fig. 7B). Expression of TH could be seen in a subset of cells, indicating that terminal differentiation of dopaminergic neurons was underway (data not shown). About 30% of total cells expressed neuronal markers such as TuJ1 and Map2ab (Fig. 6A). Thus, α-synuclein over-expression could be achieved in these cultures, but clearly induced acute toxicity to these differentiating neural progenitor cells.

Dopamine synthesis and FGF8/SHH specification of neuronal cultures contribute to acute toxicity in response to α-synuclein over-expression

We next sought to determine what factors specifically render these neuronal cell cultures sensitive to α-synuclein toxicity. As dopamine has been proposed to mediate α-synuclein toxicity (33), we tested whether α-methyl-p-tyrosine (αMT), an inhibitor of dopamine synthesis, would reduce the observed cytotoxicity. Without treatment, we obtained a similar response to α-synuclein over-expression, with 33.5 ± 0.9% (αSyn WT), 34.2 ± 1.3% (A30P) and 37.0 ± 0.6% (A53T) of TUNEL+ cells 4 days post-infection (4 ng p24). All of these conditions resulted in significantly higher amounts of cell death than seen in the non-infected (12.2 ± 0.9%) and GFP (15.9 ± 1.1%) controls (Fig. 8A). Treatment with αMT had no effect on the non-infected and GFP controls. However, the cytotoxic effects of α-synuclein over-expression were significantly decreased, with 25.1 ± 1.7% (αSyn WT), 21.1 ± 1.6% (A30P) and 20.7 ± 1.0% (A53T) of TUNEL+ cells, confirming a role for dopamine in α-synuclein cytotoxicity.

We next examined whether cell vulnerability to α-synuclein toxic effects depend on neuroectoderm specification using FGF8 and SHH, two morphogens involved in the development of the ventral midbrain. Parallel neuronal cell populations were derived from the same hESC preparation, specified in response to either FGF8 and SHH, or FGF2 only (day 8–14 and 20–25 of differentiation). FGF2 specification produced a neuronal population very similar, in number and morphology, to FGF8/SHH. However, there was a significant reduction in the number of TH+ neurons obtained, with 29.2 ± 1.0% (FGF8/SHH) versus 19.9 ± 1.1% (FGF2 only) after 9 days of differentiation ($n = 3$, $P < 0.01$).

FGF2-specified cultures were terminally differentiated for 5 days and infected as described previously (4 ng p24). Four days after infection, we observed again a significantly higher toxicity in α-synuclein over-expressers, with 16.4 ± 0.5% (αSyn WT), 18.1 ± 1.7% (A30P) and 15.7 ± 1.5% (A53T) TUNEL+ cells, when compared with the non-infected (8.7 ± 1.1%) and GFP (10.9 ± 0.6%) controls. Nevertheless, with respect to the parallel FGF8/SHH cultures described earlier, there was a clear decrease in cytotoxicity (Fig. 8B), suggesting an effect of culture specification on neuronal vulnerability.

Both in the presence of αMT and following FGF2 specification, infection with the GFP lentiviral vector induced a detectable expression in most of the neuroepithelial/neuronal cells, confirming that culture conditions had no major effect on infection efficacy (Fig. 8C).

These results suggest that dopamine production and/or specification toward susceptible human brain regions, such as the ventral midbrain, exacerbate α-synuclein cytotoxicity.

Over-expression of α-synucleins progressively impairs the neuronal pattern of terminal differentiation

We next analyzed the effects of α-synuclein on the development of dopaminergic and GABAergic markers in long-term (3 weeks) differentiating cultures (26). Neuroepithelial cells specified with FGF8/SHH were infected with lentiviral vectors (5 ng p24) after 1 day of differentiation and maintained *in vitro* for 22 days. At 8, 15 and 22 days of differentiation, the cultures were analyzed for the expression of TH and TuJ1, to determine the percentage of dopaminergic TuJ1+ neurons. TuJ1 was used as an early indicator of neuronal differentiation. The percentage of TH+ cells among TuJ1+ neurons increased steadily from day 8 to day 22, reaching 32.7 ± 1.1 and 32.8 ± 0.8% in the cells either non-infected or infected with the GFP control virus, respectively (Fig. 9A–C). In the α-synuclein over-expressers, the proportion of TH+ neurons increased at a significantly lower rate, which was most pronounced for the A53T mutation (Fig. 9A–C): 26.0 ± 3.2% (αSyn WT), 21.2 ± 1.8% (A30P) and 16.4 ± 2.1% (A53T) of TH+/TuJ1+ neurons at day 22 of differentiation. At this stage, α-synuclein over-expression could be detected by immunocytochemistry (Fig. 6C). Thus, in addition to its acute toxic effects, α-synuclein impairs dopaminergic marker expression in maturing neuronal cultures derived from hESC.

We next quantified both TH+ and GABA+ neurons to determine whether α-synuclein over-expression had specific effects on either neuronal phenotype. After 5 days of differentiation, neuronal cultures were infected as described previously (5 ng p24) and further differentiated for 16 days. It is noteworthy that this differentiation protocol generates a subpopulation of TH+ neurons that also express GABA (25–30%

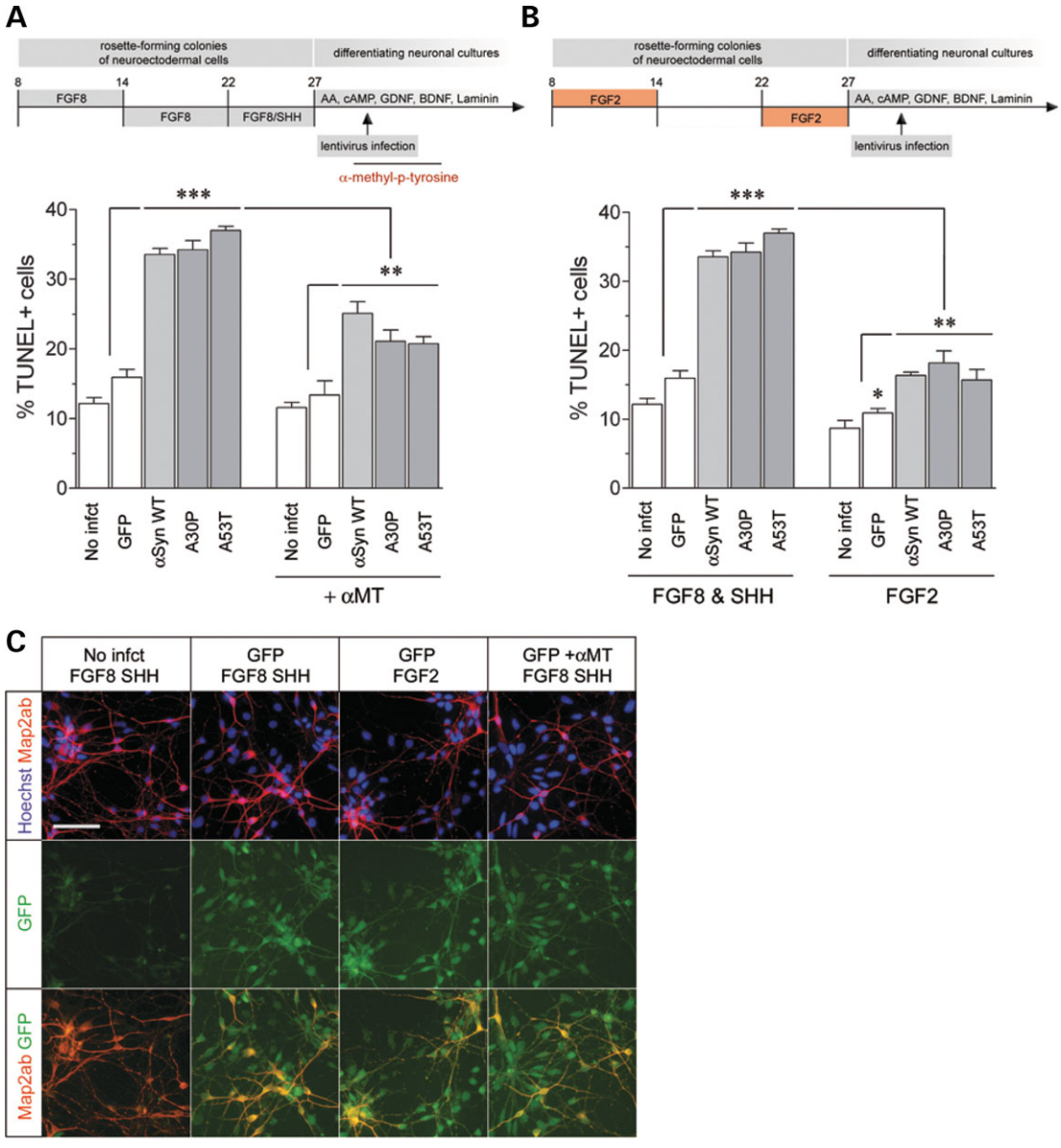

Figure 8. Inhibition of dopamine synthesis and neuroepithelial cell specification: effect on α-synuclein cytotoxicity. (**A**) Quantification of TUNEL+ cells 4 days after infection in response to α-synuclein in cells treated with αMT. $^{***}P < 0.001$ versus non-infected, GFP and αMT-treated α-synuclein over-expressers; $^{**}P < 0.01$ versus αMT-treated non-infected and GFP; $n = 3$ for each condition. (**B**) Quantification of TUNEL+ cells 4 days after infection in response to α-synuclein following FGF2 specification. $^{***}P < 0.001$ versus non-infected, GFP and FGF2-specified α-synuclein over-expressers; $^{**}P < 0.05$ versus FGF2-specified non-infected and GFP; $^{*}P < 0.05$ versus non-treated GFP; $n = 3$ for each condition. (**C**) GFP expression 4 days post lentiviral infection and immunocytochemistry for Map2ab (red). Scale bar 50 μm.

of total TH + neurons), likely with a forebrain positional identity (olfactory bulb) (26). We analyzed cells for GABA/Map2ab+ and TH/Map2ab+ co-expression to determine the percentage of neurons positive for each of these markers (Fig. 9D–E). In agreement with the previous experiment, the proportion of TH+ neurons was significantly decreased (data not shown). In contrast to TH, GABA expression was mainly affected by αSyn WT over-expression, which resulted in ∼51% loss of GABA+ neurons. Interestingly, there was less effect on GABA+ neurons with the other two mutations (Fig. 9D; A30P: 30% loss, $P < 0.05$; A53T: 22% loss, $P < 0.05$ versus GFP only). Thus, over-expression of α-synucleins impairs both the survival and maturation of neuronal cells derived from hESC, with dopaminergic and GABAergic markers being differentially affected as a function of α-synuclein forms.

DISCUSSION

PD, such as other neurodegenerative disorders, affects mainly the human species. Although neurodegeneration might result from the prolongation of the human life span, human neurons are likely to have developed unique features increas-

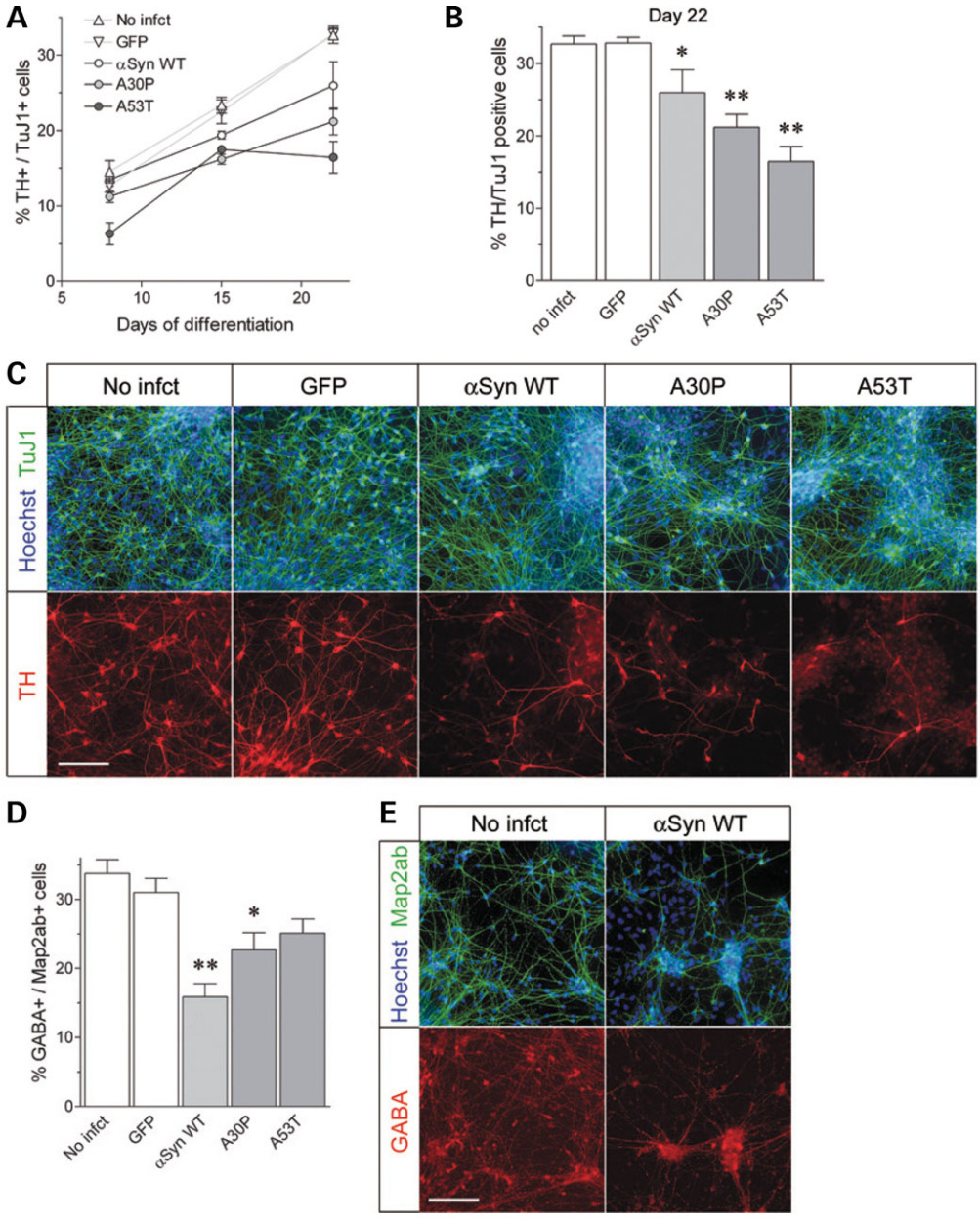

Figure 9. Pattern of differentiating neuronal subtypes. (**A**) Percentage of TH+ neurons over total TuJ1+ neurons, as a function of differentiation time, and in response to over-expression of α-synuclein and its mutants. (**B**) The same data at day 22 of differentiation. $^{*}P < 0.01$; $^{**}P < 0.001$; $n = 3$ for each condition, two-way ANOVA. (**C**) Immunocytochemistry for TuJ1 (green) and TH (red) in neuronal cultures derived from hESC and terminally differentiated for 22 days (21 days post-lentiviral infection). Scale bar 100 μm. (**D**) Bar graph showing the percentage of GABA+ neurons over total Map2ab+ neurons at day 21 of differentiation. $^{**}P < 0.01$, $^{*}P < 0.05$; $n = 3$ for each condition. (**E**) Immunocytochemistry for Map2ab (green) and GABA (red) in hESC-derived neuronal cultures terminally differentiated for 21 days (16 days post-lentiviral infection). Scale bar 100 μm.

ing their susceptibility to degeneration (34). We have developed a system for α-synuclein over-expression in human embryonic neural progenitors. Over-expression of the A53T mutant is overtly toxic, while the wild-type form impairs the normal transition of progenitors from neuronal production toward glial cell production. In hESC-derived cultures, which can produce subsets of long-projection neurons that resemble ventral midbrain dopaminergic neurons, all forms of α-synuclein induce acute cytotoxicity. This effect depends both on epigenetic progenitor specification and dopamine synthesis, and impairs the expression pattern of dopaminergic and GABAergic markers upon terminal differentiation.

Over-expression of α-synuclein in hNPC^{ctx} leads to toxicity and reduced gliogenesis

Alpha-synuclein has been over-expressed in fetal cortical progenitors to monitor its effect on their neurogenic potential. The wild-type α-synuclein form delays the normal switch to gliogenesis observed in these cultures. Both the A30P and the

A53T mutations have specific effects when compared with the wild-type form: the former enhancing gliogenesis and the latter inducing acute toxicity. These effects have rather minor amplitude when compared with the consistent toxicity observed on terminally differentiated dopaminergic neurons. Considering the adult onset of autosomal dominant forms of PD, it is unlikely that the consequence of mutations on progenitors is a primary cause of the pathology. Nevertheless, the way human cortical progenitor cells respond to these pathogenic molecules might be a good indicator of pathogenic events occurring in post-mitotic neurons and glia.

From an evolutionary standpoint, the α-*Synuclein* gene presents a remarkable adaptation. In most vertebrates, a threonine is present at the position 53. However, in Old World monkeys and humans, position 53 of the α-*Synuclein* gene encodes an alanine (35). Back mutation to a threonine in the human protein induces an early-onset dominant form of PD—the A53T mutation (2). Why rodents and other vertebrates can tolerate this mutation is not known. The acute cytotoxicity of the A53T mutant using $hNPC^{ctx}$ and other studies using human cells (33,36) demonstrate that species specificities could have increased the vulnerability of the human brain to this mutation. All $hNPC^{ctx}$ cultures infected with the A53T mutant show limited transgene expression levels when compared with the wild-type form, suggesting a lower tolerance threshold of progenitors to α-synuclein A53T.

Studies in over-expressing and knock-out mice proposed a role for α-synuclein at nerve terminals in the formation/maintenance of synaptic vesicles (10,37). But this protein has other functions yet to be explored. For example, α-synuclein is expressed during development in the mouse (38), rat (39) and human brain (7–9). While knock-out mice and over-expressers do not reveal any developmental defects, this may in part be related to the species differences discussed above.

The possible role for α-synuclein in the transition from human progenitors to mature neurons has not yet been explored. While α-synuclein is almost exclusively present in nerve terminals during adulthood, it has been found in the perikarya during development (8,9). This change in subcellular localization indicates that α-synuclein function may evolve as neural differentiation and maturation progresses. We show here that $hNPC^{ctx}$ express α-synuclein, although at a low level. When over-expressed, the protein accumulates both at cytoplasmic microvesicles and in the cell nucleus. This nuclear localization is reminiscent of initial studies that discovered the protein in neurons of the *Torpedo* electric organ, both at synaptic terminals and in the nucleus ('syn-nuclein') (40). Alpha-synuclein has been found associated with histone proteins (41) and affects both their acetylation and expression levels (41–44). With normal aging, α-synuclein accumulates in the cell soma (45), and forms Lewy bodies in diseased brain. Clustering around microvesicles might represent an early step leading to the formation of these inclusions, which contain both lipids and proteins (46). Aberrant α-synuclein localization in adult neurons might be due to elevated expression and may improperly re-activate a cell response normally driving the transition from progenitors to immature neurons. Whether this is part of the disease process will require further investigation.

When induced to differentiate, early passage $hNPC^{ctx}$ that constitutively over-express α-synuclein produce neurons at a normal rate. However, the reduced production of astrocytic cells at later passages suggests that α-synuclein impairs the normal transition to gliogenesis. Factors inducing the switch to glial cell production are still poorly understood. EGFR level controls the timing of astrogliogenesis (47), triggered by an autoregulatory activation of the JAK-STAT signaling pathway (48). How α-synuclein maintains $hNPC^{ctx}$ in their neurogenic stage remains unclear. Nevertheless, its intracellular distribution changes over time, cytoplasmic accumulation coinciding with impaired gliogenesis (Fig. 5B). Progenitors expressing the A30P mutant, with a more pronounced nuclear localization over time, consistently produce more glial cells than the wild-type form. The effect of α-synuclein on the neural/glial fate of progenitors may thus depend on its cellular distribution between the membrane/cytoplasmic/nuclear compartments. As α-synuclein could function as a physiological regulator of enzymes, transporters and vesicle formation, one can speculate a stabilizing effect on pro-neurogenic signaling pathways at the expense of the pro-gliogenic ones, thereby decreasing the proliferation rate of gliogenic progenitors. Possible interactions with the DNA matrix, as suggested by its association with histone proteins, might also influence gene transcription pattern and fate of progenitor cells. Important physiological effects on $hNPC^{ctx}$ prior to differentiation into neurons, lends further credence to a widespread effect of α-synuclein over-expression and not just at the synapse.

Alpha-synuclein and its mutants induce acute toxicity in hESC-derived neuronal cultures that is sensitive to dopamine and neurodevelopmental specification

PD is a progressive disorder that affects multiple neuronal subtypes. As proposed recently, the disease could initially affect enteric (49) and cardiac sympathetic innervations, propagate into the central nervous system via the brainstem and the olfactory bulb, and spread into the ventral midbrain dopaminergic system, locus cœruleus and cerebral cortex (50). However, degeneration of long-projection dopaminergic neurons in the *substantia nigra pars compacta* remains a prominent feature that leads to some of the most severe symptoms.

Both mouse and human ES cells can be efficiently differentiated into neuroepithelial cells, further specified into dopaminergic long-projection neurons (25,26,51,52). As such, they provide a flexible source of cells that can be used to develop *in vitro* models of PD. Using mouse ES cells, this approach has already been explored by over-expressing α-synuclein (53). In both cases, additional exposure to oxidative stress and proteasome inhibition is needed to reveal increased cell vulnerability. Alpha-synuclein also leads to neuronal loss in response to prolonged cell culture.

In order to generate cells with selective vulnerability to α-synuclein, we have used neuroepithelial cells derived from hESC, and specified using SHH and FGF8. This culture system is still immature, and does not reproduce all the connectivity and cell extrinsic factors specific to the adult *substantia nigra*. Nevertheless, it provides a source of non-

transformed human neuronal cells that synthesize dopamine and have been specified using the factors that govern the development of the ventral midbrain (54). We have observed an acute toxicity of α-synuclein *per se* at low viral doses with a PGK promoter system driving mid-level expression. As expected, all three forms of α-synuclein are toxic, including the wild-type form, whose additional gene copies induce dominant PD. Clearly, differentiating human neuronal cultures are highly vulnerable to α-synuclein without the need for any additional stress. This susceptibility is linked to specific cellular conditions, since inhibition of TH, the rate-limiting enzyme in dopamine synthesis and neurectoderm specification using FGF2, which shifts the pattern of neuronal subtypes produced, both reduce cytotoxicity. Alpha-synuclein induces death in human progenitors developing into long projection neurons, at a stage where the cells have not established organized synapses yet, in a large fraction of cells that goes beyond the population of TH+ neurons. It is unclear whether the progressive decrease in the proportion of TH+ and GABA+ neurons in response to α-synuclein reflects a selective cytotoxicity (33,55) or a reduction in the differentiation of neuronal sub-types. Interestingly, α-synuclein over-expression has been shown to directly affect TH expression, suggesting possible direct effects on the presence of these neuronal markers (56).

Towards the development of *in vitro* models of neurodegeneration in human cells

In vitro models based on human progenitor cells might complement the genetic animal and cell models recently established. Ideally, a human cell model should be based on mutations with a causative role demonstrated in patients, and recapitulate pathological features such as protein aggregation and progressive neuronal dysfunction and/or death. With the growing number of mutations discovered, genetic models are now proposed for most neurodegenerative disorders, including Alzheimer's disease, PD, Huntington's disease and amyotrophic lateral sclerosis. Fetal and embryonic stem cells could be derived from human samples carrying the mutations or generated by nuclear transfer from adult donor cells (57). However, ethical concerns and technical hurdles still limit the derivation of these cells and it remains unclear whether culture conditions and exogenous stress will accelerate a pathogenesis that normally develops over decades. Viral gene transfer constitutes a flexible system to induce stable transgene integration in a high percentage of cells, and control both the time and level of expression. Although this approach still needs refinement to better recapitulate the progressive degeneration and the time-dependent protein aggregation, it paves the way for the design of hESC-based cell technologies as a tool to dissect neurodegeneration and screen for therapeutics.

MATERIALS AND METHODS

Lentiviral vector production and titration

Vesicular stomatitis virus G (VSV-G)-pseudotyped lentiviruses were produced by transient calcium phosphate cotransfection of 293T cells as described previously (58). Lentiviral vector concentrations were initially normalized according to the p24 (HIV-1 capsid protein) content of supernatants measured by enzyme-linked immunosorbent assay. Ten-times concentrated stocks of lentiviruses were used for cell infection.

To obtain a better assessment of the infectious viral particles, viral genomes were titered using a RT-qPCR protocol adapted from the method of Lizee *et al.* (59). Lentiviral vector particles quantified by ELISA for the p24 viral coat protein were suspended in PBS at a concentration of 1000 ng p24/ml. Two 10-fold serial dilutions were made in PBS and RNA was isolated using the RNeasy kit (Qiagen, Germany) according to the manufacturer's protocol including the optional DNase step. Reverse transcription was performed using random hexamer primers and Superscript III RT (Invitrogen, Carlsbad, CA, USA), according to the manufacturer's protocol. Taqman assays were performed in triplicate using 2 μl template cDNA, Taqman Universal master mix (Applied Biosystems, Inc, Foster City, CA, USA), primers and probe for WPRE (see below). A standard curve was constructed using the virus shuttle vector plasmid as template and used to calculate relative RNA content. Viral p24 titers were adjusted to reflect the amount of RNA present in each viral preparation.

Cell culture

Culture of hNPC^{ctx} Human fetal cortical progenitor cells (hNPC^{ctx}) were isolated by dissection from post mortem brain tissue from the following donors: M006, male at 87 days of gestation; M031, male at 94 days of gestation; M045, male at 91 days of gestation; M046, male, 87 days of gestation. The methods of collection conform to the National Institutes of Health guidelines and University of Wisconsin Institutional Review Board requirements for the collection of such tissue. Human NPC^{ctx} were cultured in 70% DMEM (high glucose, supplemented with l-glucosamine), 30% Ham's F-12, 1% antibiotic-antimycotic, 2% B27 (all from Invitrogen), 20 ng/ml EGF (Sigma, St Louis, MO, USA), 20 ng/ml FGF2 (R&D Systems, Inc., Minneapolis, MN, USA) and 5 mg/ml heparin (Sigma) for 4 weeks after which the FGF2, heparin and B27 were removed and 1% N2 (Invitrogen) was added. Neurosphere aggregates were maintained at 200 μm by chopping with a McIlvain tissue chopper (Vibratome, St Louis, MO, USA) when the majority of the spheres in culture reached a diameter $\geq$0.5 mm. Progenitors were maintained at a density of $5x10^5$ cells/ml of medium, half of the medium being replaced with fresh medium every 3 days. Unless stated otherwise, 10 ng/ml leukemia inhibitory factor (LIF; Chemicon, Temecula, CA, USA) was added to the media after 10–15 weeks in culture.

Differentiation of hNPC^{ctx} For differentiation, spheres were collected by gravity sedimentation, washed three times with basal media (no growth factors) and resuspended in plating media (DMEM/F-12, 2% B27). Whole spheres were adhered to laminin-coated plastic and allowed to differentiate in plating media for 7–10 days. During differentiation, half of the plating medium was replaced every 2 days with fresh

medium. To facilitate cell immunostaining and counting, the differentiated cultures were detached by a 5 min Accutase (Chemicon) treatment, washed to remove enzyme and replated on glass coverslips coated with poly-L-lysine and laminin. After a brief incubation for 2–4 h in Neurobasal medium (Invitrogen) supplemented with 1 mM l-glutamine, 2% B27 and 1% fetal bovine serum (FBS) for cell adhesion, the cultures were fixed in 4% paraformaldehyde for immunocytochemistry. Alternatively, neurospheres were dissociated 10 min with Accutase, washed for enzyme removal and plated on glass coverslips, at an initial density of 50 000 cells per coverslip. After 7 days of differentiation, the cultures were fixed for immunostaining and counting.

Infection of hNPC^{ctx} Neurospheres were collected 5 days post-passaging and allowed to settle by gravity. Media was removed and spheres resuspended in one ml Accutase per 10 million cells, mixed gently and incubated at 37°C for 10 min. Accutase was replaced with an equal volume of 0.2% trypsin inhibitor (Sigma) and the cells were washed three times in 10 ml media. Cells were gently dissociated by trituration, counted on a hemacytometer and suspended in conditioned media at 1000 cells/μl. 300 000 cells were plated per well of a 24-well plate (minimum 10 wells) and mixed with virus diluted to the desired titer in 100 μl of fresh media. Cells were exposed to a viral concentration of 75 ng p24/ml. Cells were allowed to re-associate in the presence of virus and 24–72 h later, small spheres were collected and seeded into flasks at a density of 500 000 cells/ml. Transgenic spheres were expanded for 1 month after which molecular analysis was performed.

Culture of hESC Human ESC (H9 line, NIH registry WA09) were cultured on a feeder layer of irradiated mouse embryonic fibroblasts and passaged weekly as described previously (23). Differentiated colonies were physically removed before passaging.

Culture, differentiation and infection of neuroectodermal cells This procedure has been described previously (26). Colonies of hESC were detached from the feeder layer by a brief exposure to dispase 1 mg/ml (Invitrogen) and cultured as cell aggregates in suspension (embryoid bodies) for 4 days in regular culture medium without FGF2. On day 4, embryoid bodies were transferred to neural induction medium (DMEM/F12 1:1 (Invitrogen), 1% N2 supplement, 2 μg/ml heparin and 10 ng/ml FGF2). After 3 days, cells were induced to adhere in the six-well plates in the presence of 10% FBS and on day 4, the neural induction medium was supplemented with 50 ng/ml FGF8 (PeproTech, Rocky Hill, NJ, USA) instead of FGF2, unless stated otherwise. Ten days after initiation of the differentiation process, colonies started to differentiate into neuroectodermal cells displaying columnar morphology with an organization into neural tube-like rosettes. Colonies were grown for 6 days in this medium and then mechanically detached from the surrounding cells for culture in suspension. Half of the medium was replaced every other day and once neurospheres formed, they were mechanically broken using a Pasteur pipette to facilitate their expansion in small clusters. Non-neuroectodermal colonies were identified by cell morphology and removed from the culture. After 6–10 days, 40 ng/ml of human SHH (C24II amino terminal peptide, R&D systems, Inc.) was added to the medium for 5 additional days. Finally, the neurospheres were carefully dissociated in Accutase, and 30 000 cells plated on glass coverslips coated with poly-L-lysine and laminin for terminal differentiation. The cells were maintained in Neurobasal medium (Invitrogen), supplemented with 2% B27, 1% non-essential amino acids solution (Invitrogen), 1% antibiotic-antimycotic, 0.5 mM l-glutamine, 1 μg/ml laminin, 1 μM cyclic AMP, 200 μM ascorbic acid, 10 ng/ml BDNF (PeproTech) and 10 ng/ml GDNF (R&D Systems, Inc.). Half of the culture medium was changed every other day. At this stage, the cultures were infected with lentiviral vectors (4–5 ng of p24) in 300 μl medium (viral concentration = 13–17 ng p24/ml).

Immunocytochemistry and microscopy Cultures were fixed in 4% paraformaldehyde for 20 min at room temperature and washed in PBS. Fixed cells were blocked in 5% goat or donkey serum and permeabilized using 0.2% Triton X-100. Primary antibodies used included monoclonal antibodies directed against α-synuclein LB509 (1:200; Zymed), Map2ab (1:250; Sigma), βIII-tubulin (TuJ1, clone SDL.3D10, 1:3000; Sigma) and rabbit polyclonal antibodies directed against GFAP (1:1000; DakoCytomation, Denmark), GABA (1:2000; Sigma), Ki67 (1:1000; NovoCastra, UK), Nestin (AB5922, 1:5000; Chemicon) and TH (1:500; Pel-Freez, Rogers, AR, USA). Secondary antibodies used were goat-anti mouse IgG2b AF488 (Molecular Probes, Invitrogen), donkey anti-rabbit Cy3 (Jackson Immunoresearch, West Grove, PA, USA), donkey anti-mouse Cy3 (Jackson) and goat anti-rabbit AF546 (Molecular Probes). Nuclei were stained with the Hoechst 33258 dye. Images were collected using the SPOT Advanced software (Diagnostic Instruments Inc., Burroughs Street, MI, USA) and a SPOT digital camera mounted on a Nikon microscope E600 equipped with epifluorescence. Cell counts were performed with the Metamorph imaging software (Universal Imaging, Downingtown, PA, USA) by an observer blind to the experimental conditions.

Cell proliferation and cell death assays The rate of progenitor cell division was determined either by Ki67 staining (see above) or BrdU pulse labeling. Briefly, hNPC^{ctx} grown as neurospheres were collected, dissociated with Accutase, replated at a density of 50 000 cells in 50 μl on a glass coverslip coated with poly-L-lysine and laminin, and grown in the regular culture medium supplemented with EGF and LIF. Three days later, the cells were pulsed with 0.2 μM BrdU (Sigma) for 14 to 40 h, depending on their growth rate. The cells were fixed in ice-cold methanol, blocked in 5% donkey serum and permeabilized with 0.2% Triton X-100. Cells having incorporated BrdU were immunostained with rat anti-BrdU antibodies (1:500; Accurate Chemical & Scientific Corporation, Westbury, NY, USA) and goat anti-rat Cy3 secondary antibodies (Jackson). Cell fluorescence analysis was performed as described above and the proliferation rate of the cells was expressed as the percentage of Ki67+ or BrdU+ nuclei over the total number of nuclei stained with Hoechst 33258.

The rate of cell death in cultures of $hNPC^{ctx}$ and differentiated hESC was determined using *in situ* fluorescent TUNEL staining (Roche Diagnostics GmbH, Mannheim, Germany), according to manufacturer's protocol. Briefly, cells plated on glass coverslips were fixed in 4% paraformaldehyde, blocked and permeabilized as described earlier. TUNEL labeling was performed for 40 min at 37°C and the cells were subsequently immunostained for α-synuclein or TH. Cell fluorescence analysis was performed as described previously and the rate of cell death expressed as the percentage of TUNEL+ cells over the total number of nuclei stained with Hoechst 33258.

Protein analysis Neurospheres were isolated, suspended in 1% Triton X-100 lysis buffer supplemented with 1% protease inhibitor cocktail (P8340, Sigma), triturated and centrifuged at 13 000 rpm for 10 min at 4°C. In some experiments, nuclear and cytoplasmic protein extracts were obtained using the NE-PER reagents (Pierce, Rockford, IL, USA) following manufacturer's protocol. Protein concentration was determined using the DC protein assay (Biorad, Richmond, VA, USA). Ten to twenty micrograms of proteins were separated on 12 or 15% SDS-polyacrylamide gel, and electro-transferred to nitrocellulose membrane. The membrane was blocked with 5% dry milk in Tris-buffered saline containing 0.1% Tween 20 and probed with primary antibodies toward α-synuclein (AB5038 rabbit polyclonal, 1:2000, Chemicon; LB509, 1:500, Zymed, San Francisco, CA; Syn204, 1:1000, Lab Vision, Fremont, CA) and α-actin (monoclonal, 1:1000, Sigma) and then incubated with either anti-mouse or anti-rabbit secondary antibodies conjugated to horseradish peroxidase (Promega, Madison). Antibody labeling was visualized using the ECL chemiluminescence kit (Amersham, Piscataway, NJ, USA). For semi-quantitative analysis, signal intensity was analyzed with the Metamorph imaging software (Universal Imaging) and corrected with respect to the α-actin loading control.

Immunoprecipitation was performed using sepharose-protein G beads (Amersham) according to manufacturer's protocol. Three micrograms of anti-α-synuclein antibodies (Syn211, Zymed) were incubated with a neurosphere cell lysate. After elution, the total protein extract was analyzed by western blotting using the LB509 antibody as described previously.

Quantitative PCR Taqman qPCR was performed on an Opticon 2 (MJ Research, Inc., Waltham, MA, USA) using Taqman Universal PCR Master mix (Applied Biosystems, Inc.) and FAM-labeled probes. Genomic DNA was isolated from neurospheres using DNeasy kit (Qiagen) and 100 ng per reaction was used as template. RNA was isolated from neurospheres using RNeasy kit (Qiagen) and reverse transcription reactions were performed as described for viral titering, except that 1 μg of RNA was used for each RT reaction. One tenth of the total cDNA was used as a template for qPCR amplification. Standard curves were constructed using serial dilutions of a plasmid containing WPRE and GDNF transgene sequences or serial dilutions of genomic DNA for albumin or cDNA for β-actin. When needed, reaction efficiencies were taken into account for quantification of sequence abundance (WPRE: 1.96; albumin: 2.00; β-actin: 1.99).

Sequence of primers and probes used were:

WPRE: forward 5'-CCGTTGTCAGGCAACGTG-3'
reverse 5'-AGCTGACAGGTGGTGGCAAT-3'
probe 5'-FAM-TGCTGACGCAACCCCCACTGGT-TAMRA-3'
Albumin: forward 5'-TGAAACATACGTTCCCAAAGAGTTT-3'
reverse 5'-CTCTCCTTCTCAGAAAGTGTGCATAT-3'
probe 5'-FAM-TGCTGAAACATTCACCTTCCATGCAGA-TAMRA-3'
β-actin: forward 5'-GCGAGAAGATGACCCAGATC-3'
reverse 5'-CCAGTGGTACGGCCAGAGG-3'
probe 5'-FAM-CCAGCCATGTACGTTGCTATCCAGGC-TAMRA-3'

Electron microscopy

Initial sample preparation Fresh cell cultures were fixed on their glass coverslips in 4% paraformaldehyde, 0.1% glutaraldehyde in 0.1M Sorenson's Sodium Phosphate buffer (PB, pH = 7.4) for 30 min at room temperature. All antibody and silver enhancing treatments were carried out on a shaker table at room temperature, unless stated otherwise.

Antibody treatment Following fixation, the cells were rinsed in 0.1M PB, and treated with freshly prepared 0.1% sodium borohydride in 0.1M PB for 10 min to quench unbound aldehydes. Next, the cells were permeabilized for 30 min with 0.1% Triton X-100 in phosphate buffered saline (PBS, 10 mM Phosphate buffer, 150 mM NaCl, pH = 7.4) followed by three 10 min rinses in PBS. The cells were then blocked for non-specific antibody binding with Aurion Goat Blocking Agent (containing 5% BSA, 0.1% Cold Water Fish Gelatin and 5% normal goat serum in PBS, pH 7.4; Aurion, The Netherlands) for 30 min. The cells were then rinsed three times for 10 min each in incubation buffer (IB) containing PBS + 0.1% BSA-C (Aurion Immuno Gold Reagents). Finally, the samples were incubated in a mixture of IB and rabbit anti-α-synuclein at a dilution of 1:500 overnight at 4°C. The following day, the cells were rinsed in IB every 10 min for 2 h (12 rinses total), then incubated overnight in a 1:100 dilution of Ultra Small gold conjugate F(ab') 2 fragment of goat-anti-rabbit IgG (H&L) (Aurion Immuno Gold Reagents) at 4°C. After the overnight incubation, the cells were rinsed in IB, 6 × 10 min, and rinsed in PBS 6 × 5 min. The cells were post-fixed in 2% glutaraldehyde in 0.1M PB for 30 min, and rinsed 2 × 5 min in PB.

Silver enhancement The use of Ultra Small gold conjugates requires a silver-enhancing step to increase the size of the sub-nanometer gold particles in order to visualize more easily the particles by TEM. After post fixation, the cells were rinsed 3 × 10 min in Enhancing Conditioning Buffer (ECS, Aurion Immuno Gold Reagents). Next the cells were developed in Silver Enhancement Solution (Aurion Immuno Gold Reagents) for 1.25 h. To terminate silver enhancement, the cells were exposed to a solution of 0.3 M sodium thiosulfate

in ECS for 5 min. The samples were then rinsed 2 × 10 min in ECS and finally processed routinely for TEM.

Routine electron microscopy processing After silver enhancing, the cells were fixed in a solution of 1.0% osmium tetroxide in 0.1M PB for 30 min. Following OsO4 post-fixation, the samples were dehydrated in a graded ethanol series, transitioned in propylene oxide and infiltrated in PolyBed/812 (Polysciences, Inc., Warrington, PA, USA) epoxy resin. The infiltrated cell populated coverslips were flat-embedded, cell side up in Al weighing dishes and polymerized for 48 h at 60°C.

Ultrathin sectioning After polymerization, the embedded coverslips were removed from the Al dishes. The excess hardened resin was scraped off the non-cell side, and the glass dissolved away in Hydrofluoric acid. After extensive distilled water rinsing, the samples were sectioned for TEM using a Reichert-Jung Ultracut-E Ultramicrotome, and contrasted with Reynolds lead citrate and 8% uranyl acetate in 50% EtOH. Ultrathin sections were observed with a Philips CM120 or a JEOL 100CX electron microscope (80 kV) and images were captured with a SIS MegaView III (Soft Imaging Systems, Lakewood, CO, USA) side-mounted digital camera.

Statistical analysis Unless stated otherwise, data are expressed as means ± SEM. For quantification of cell death, cell proliferation and immunolabelings, cell counts were performed on 3 to 4 independent experiments. For each experiment, at least 1,000 cells total were counted on 5 fields per coverslip. Data were analyzed using a one- or two-way analysis of variance (ANOVA) followed by a Newman-Keuls post hoc test on the Prism software (GraphPad Software, Inc., San Diego, CA, USA). P-values < 0.05 were considered as statistically significant.

SUPPLEMENTARY MATERIAL

Supplementary Material is available at HMG Online.

ACKNOWLEDGEMENTS

We are grateful to Jacalyn McHugh, Huafang Lai, Caroline Zieth and Kyle Wallace for their expert technical help and to Dr Romain Zufferey, Viviane Padrun and Fabienne Pidoux for virus production. We also thank Drs Anita Bhattacharyya, David Gamm, Zhi Jian Zhang and Xue-Jun Li for their scientific support and Randall J. Massey for his expert technical help at the electron microscope facility of the UW-Madison Medical School.

BLS is supported by the Swiss Foundation for Grants in Biology and Medicine. We are also grateful to the UW Foundation for his support.

Conflict of Interest statement. None declared.

REFERENCES

1. Kruger, R., Kuhn, W., Muller, T., Woitalla, D., Graeber, M., Kosel, S., Przuntek, H., Epplen, J.T., Schols, L. and Riess, O. (1998) Ala30Pro mutation in the gene encoding alpha-synuclein in Parkinson's disease. *Nat. Genet.*, **18**, 106–108.
2. Polymeropoulos, M.H., Lavedan, C., Leroy, E., Ide, S.E., Dehejia, A., Dutra, A., Pike, B., Root, H., Rubenstein, J., Boyer, R. *et al*. (1997) Mutation in the alpha-synuclein gene identified in families with Parkinson's disease. *Science*, **276**, 2045–2047.
3. Zarranz, J.J., Alegre, J., Gomez-Esteban, J.C., Lezcano, E., Ros, R., Ampuero, I., Vidal, L., Hoenicka, J., Rodriguez, O., Atares, B. *et al*. (2004) The new mutation, E46K, of alpha-synuclein causes Parkinson and Lewy body dementia. *Ann. Neurol.*, **55**, 164–173.
4. Ibanez, P., Bonnet, A.M., Debarges, B., Lohmann, E., Tison, F., Pollak, P., Agid, Y., Durr, A. and Brice, A. (2004) Causal relation between alpha-synuclein gene duplication and familial Parkinson's disease. *Lancet*, **364**, 1169–1171.
5. Singleton, A.B., Farrer, M., Johnson, J., Singleton, A., Hague, S., Kachergus, J., Hulihan, M., Peuralinna, T., Dutra, A., Nussbaum, R. *et al*. (2003) alpha-Synuclein locus triplication causes Parkinson's disease. *Science*, **302**, 841.
6. Spillantini, M.G., Crowther, R.A., Jakes, R., Hasegawa, M. and Goedert, M. (1998) alpha-Synuclein in filamentous inclusions of Lewy bodies from Parkinson's disease and dementia with lewy bodies. *Proc. Natl. Acad. Sci. USA*, **95**, 6469–6473.
7. Bayer, T.A., Jakala, P., Hartmann, T., Egensperger, R., Buslei, R., Falkai, P. and Beyreuther, K. (1999) Neural expression profile of alpha-synuclein in developing human cortex. *Neuroreport*, **10**, 2799–2803.
8. Galvin, J.E., Schuck, T.M., Lee, V.M. and Trojanowski, J.Q. (2001) Differential expression and distribution of alpha-, beta-, and gamma-synuclein in the developing human substantia nigra. *Exp. Neurol.*, **168**, 347–355.
9. Raghavan, R., Kruijff, L., Sterrenburg, M.D., Rogers, B.B., Hladik, C.L. and White, C.L., 3rd. (2004) Alpha-synuclein expression in the developing human brain. *Pediatr. Dev. Pathol.*, **7**, 506–516.
10. Abeliovich, A., Schmitz, Y., Farinas, I., Choi-Lundberg, D., Ho, W.H., Castillo, P.E., Shinsky, N., Verdugo, J.M., Armanini, M., Ryan, A. *et al*. (2000) Mice lacking alpha-synuclein display functional deficits in the nigrostriatal dopamine system. *Neuron*, **25**, 239–252.
11. Outeiro, T.F. and Lindquist, S. (2003) Yeast cells provide insight into alpha-synuclein biology and pathobiology. *Science*, **302**, 1772–1775.
12. Lakso, M., Vartiainen, S., Moilanen, A.M., Sirvio, J., Thomas, J.H., Nass, R., Blakely, R.D. and Wong, G. (2003) Dopaminergic neuronal loss and motor deficits in Caenorhabditis elegans overexpressing human alpha-synuclein. *J. Neurochem.*, **86**, 165–172.
13. Feany, M.B. and Bender, W.W. (2000) A Drosophila model of Parkinson's disease. *Nature*, **404**, 394–398.
14. Giasson, B.I., Duda, J.E., Quinn, S.M., Zhang, B., Trojanowski, J.Q. and Lee, V.M. (2002) Neuronal alpha-synucleinopathy with severe movement disorder in mice expressing A53T human alpha-synuclein. *Neuron*, **34**, 521–533.
15. Lee, M.K., Stirling, W., Xu, Y., Xu, X., Qui, D., Mandir, A.S., Dawson, T.M., Copeland, N.G., Jenkins, N.A. and Price, D.L. (2002) Human alpha-synuclein-harboring familial Parkinson's disease-linked Ala-53 –> Thr mutation causes neurodegenerative disease with alpha-synuclein aggregation in transgenic mice. *Proc. Natl. Acad. Sci. USA*, **99**, 8968–8973.
16. van der Putten, H., Wiederhold, K.H., Probst, A., Barbieri, S., Mistl, C., Danner, S., Kauffmann, S., Hofele, K., Spooren, W.P., Ruegg, M.A. *et al*. (2000) Neuropathology in mice expressing human alpha-synuclein. *J. Neurosci.*, **20**, 6021–6029.
17. Kirik, D., Rosenblad, C., Burger, C., Lundberg, C., Johansen, T.E., Muzyczka, N., Mandel, R.J. and Bjorklund, A. (2002) Parkinson-like neurodegeneration induced by targeted overexpression of alpha-synuclein in the nigrostriatal system. *J. Neurosci.*, **22**, 2780–2791.
18. Lo Bianco, C., Ridet, J.L., Schneider, B.L., Deglon, N. and Aebischer, P. (2002) alpha -Synucleinopathy and selective dopaminergic neuron loss in a rat lentiviral-based model of Parkinson's disease. *Proc. Natl. Acad. Sci. USA*, **99**, 10813–10818.
19. Kirik, D., Annett, L.E., Burger, C., Muzyczka, N., Mandel, R.J. and Bjorklund, A. (2003) Nigrostriatal alpha-synucleinopathy induced by viral vector-mediated overexpression of human alpha-synuclein: a new primate model of Parkinson's disease. *Proc. Natl. Acad. Sci. USA*, **100**, 2884–2889.

20. Jakel, R.J., Schneider, B.L. and Svendsen, C.N. (2004) Using human neural stem cells to model neurological disease. *Nat. Rev. Genet.*, **5**, 136–144.
21. Svendsen, C.N., ter Borg, M.G., Armstrong, R.J., Rosser, A.E., Chandran, S., Ostenfeld, T. and Caldwell, M.A. (1998) A new method for the rapid and long term growth of human neural precursor cells. *J. Neurosci. Methods*, **85**, 141–152.
22. Wright, L.S., Prowse, K.R., Wallace, K., Linskens, M.H. and Svendsen, C.N. (2006) Human progenitor cells isolated from the developing cortex undergo decreased neurogenesis and eventual senescence following expansion *in vitro*. *Exp. Cell Res.*, **312**, 2107–2120.
23. Thomson, J.A., Itskovitz-Eldor, J., Shapiro, S.S., Waknitz, M.A., Swiergiel, J.J., Marshall, V.S. and Jones, J.M. (1998) Embryonic stem cell lines derived from human blastocysts. *Science*, **282**, 1145–1147.
24. Li, X.J., Du, Z.W., Zarnowska, E.D., Pankratz, M., Hansen, L.O., Pearce, R.A. and Zhang, S.C. (2005) Specification of motoneurons from human embryonic stem cells. *Nat. Biotechnol.*, **23**, 215–221.
25. Perrier, A.L., Tabar, V., Barberi, T., Rubio, M.E., Bruses, J., Topf, N., Harrison, N.L. and Studer, L. (2004) Derivation of midbrain dopamine neurons from human embryonic stem cells. *Proc. Natl. Acad. Sci. USA*, **101**, 12543–12548.
26. Yan, Y., Yang, D., Zarnowska, E.D., Du, Z., Werbel, B., Valliere, C., Pearce, R.A., Thomson, J.A. and Zhang, S.C. (2005) Directed differentiation of dopaminergic neuronal subtypes from human embryonic stem cells. *Stem Cells*, **23**, 781–790.
27. Li, W., West, N., Colla, E., Pletnikova, O., Troncoso, J.C., Marsh, L., Dawson, T.M., Jakala, P., Hartmann, T., Price, D.L. *et al*. (2005) Aggregation promoting C-terminal truncation of alpha-synuclein is a normal cellular process and is enhanced by the familial Parkinson's disease-linked mutations. *Proc. Natl. Acad. Sci. USA*, **102**, 2162–2167.
28. Anderson, J.P., Walker, D.E., Goldstein, J.M., de Laat, R., Banducci, K., Caccavello, R.J., Barbour, R., Huang, J., Kling, K., Lee, M. *et al*. (2006) Phosphorylation of Ser-129 is the dominant pathological modification of alpha-synuclein in familial and sporadic Lewy body disease. *J. Biol. Chem.*, **281**, 29739–29752.
29. Cole, N.B., Murphy, D.D., Grider, T., Rueter, S., Brasaemle, D. and Nussbaum, R.L. (2002) Lipid droplet binding and oligomerization properties of the Parkinson's disease protein alpha-synuclein. *J. Biol. Chem.*, **277**, 6344–6352.
30. Jensen, P.H., Nielsen, M.S., Jakes, R., Dotti, C.G. and Goedert, M. (1998) Binding of alpha-synuclein to brain vesicles is abolished by familial Parkinson's disease mutation. *J. Biol. Chem.*, **273**, 26292–26294.
31. Svendsen, C.N., Clarke, D.J., Rosser, A.E. and Dunnett, S.B. (1996) Survival and differentiation of rat and human epidermal growth factor-responsive precursor cells following grafting into the lesioned adult central nervous system. *Exp. Neurol.*, **137**, 376–388.
32. Ostenfeld, T., Joly, E., Tai, Y.T., Peters, A., Caldwell, M., Jauniaux, E. and Svendsen, C.N. (2002) Regional specification of rodent and human neurospheres. *Brain Res. Dev. Brain Res.*, **134**, 43–55.
33. Xu, J., Kao, S.Y., Lee, F.J., Song, W., Jin, L.W. and Yankner, B.A. (2002) Dopamine-dependent neurotoxicity of alpha-synuclein: a mechanism for selective neurodegeneration in Parkinson disease. *Nat. Med.*, **8**, 600–606.
34. Vernier, P., Moret, F., Callier, S., Snapyan, M., Wersinger, C. and Sidhu, A. (2004) The degeneration of dopamine neurons in Parkinson's disease: insights from embryology and evolution of the mesostriatocortical system. *Ann. N.Y. Acad. Sci.*, **1035**, 231–249.
35. Hamilton, B.A. (2004) alpha-Synuclein A53T substitution associated with Parkinson disease also marks the divergence of Old World and New World primates. *Genomics*, **83**, 739–742.
36. Lee, M., Hyun, D., Halliwell, B. and Jenner, P. (2001) Effect of the overexpression of wild-type or mutant alpha-synuclein on cell susceptibility to insult. *J. Neurochem.*, **76**, 998–1009.
37. Chandra, S., Gallardo, G., Fernandez-Chacon, R., Schluter, O.M. and Sudhof, T.C. (2005) Alpha-synuclein cooperates with CSPalpha in preventing neurodegeneration. *Cell*, **123**, 383–396.
38. Hsu, L.J., Mallory, M., Xia, Y., Veinbergs, I., Hashimoto, M., Yoshimoto, M., Thal, L.J., Saitoh, T. and Masliah, E. (1998) Expression pattern of synucleins (non-Abeta component of Alzheimer's disease amyloid precursor protein/alpha-synuclein) during murine brain development. *J. Neurochem.*, **71**, 338–344.
39. Petersen, K., Olesen, O.F. and Mikkelsen, J.D. (1999) Developmental expression of alpha-synuclein in rat hippocampus and cerebral cortex. *Neuroscience*, **91**, 651–659.
40. Maroteaux, L., Campanelli, J.T. and Scheller, R.H. (1988) Synuclein: a neuron-specific protein localized to the nucleus and presynaptic nerve terminal. *J. Neurosci.*, **8**, 2804–2815.
41. Goers, J., Manning-Bog, A.B., McCormack, A.L., Millett, I.S., Doniach, S., Di Monte, D.A., Uversky, V.N. and Fink, A.L. (2003) Nuclear localization of alpha-synuclein and its interaction with histones. *Biochemistry*, **42**, 8465–8471.
42. Duce, J.A., Smith, D.P., Blake, R.E., Crouch, P.J., Li, Q.X., Masters, C.L. and Trounce, I.A. (2006) Linker Histone H1 Binds to Disease Associated Amyloid-like Fibrils. *J. Mol. Biol.*, **361**, 493–505.
43. Vartiainen, S., Pehkonen, P., Lakso, M., Nass, R. and Wong, G. (2006) Identification of gene expression changes in transgenic C. elegans overexpressing human alpha-synuclein. *Neurobiol. Dis.*, **22**, 477–486.
44. Kontopoulos, E., Parvin, J.D. and Feany, M.B. (2006) {alpha}-synuclein acts in the nucleus to inhibit histone acetylation and promote neurotoxicity. *Hum. Mol. Genet.*, **15**, 3012–3023.
45. Chu, Y. and Kordower, J.H. (2006) Age-associated increases of alpha-synuclein in monkeys and humans are associated with nigrostriatal dopamine depletion: is this the target for Parkinson's disease? *Neurobiol. Dis.*, **25**, 134–149.
46. Gai, W.P., Yuan, H.X., Li, X.Q., Power, J.T., Blumbergs, P.C. and Jensen, P.H. (2000) *In situ* and *in vitro* study of colocalization and segregation of alpha-synuclein, ubiquitin, and lipids in Lewy bodies. *Exp. Neurol.*, **166**, 324–333.
47. Viti, J., Feathers, A., Phillips, J. and Lillien, L. (2003) Epidermal growth factor receptors control competence to interpret leukemia inhibitory factor as an astrocyte inducer in developing cortex. *J. Neurosci.*, **23**, 3385–3393.
48. He, F., Ge, W., Martinowich, K., Becker-Catania, S., Coskun, V., Zhu, W., Wu, H., Castro, D., Guillemot, F., Fan, G. *et al*. (2005) A positive autoregulatory loop of Jak-STAT signaling controls the onset of astrogliogenesis. *Nat. Neurosci.*, **8**, 616–625.
49. Braak, H., de Vos, R.A., Bohl, J. and Del Tredici, K. (2006) Gastric alpha-synuclein immunoreactive inclusions in Meissner's and Auerbach's plexuses in cases staged for Parkinson's disease-related brain pathology. *Neurosci. Lett.*, **396**, 67–72.
50. Braak, H., Del Tredici, K., Rub, U., de Vos, R.A., Jansen Steur, E.N. and Braak, E. (2003) Staging of brain pathology related to sporadic Parkinson's disease. *Neurobiol. Aging*, **24**, 197–211.
51. Kim, J.H., Auerbach, J.M., Rodriguez-Gomez, J.A., Velasco, I., Gavin, D., Lumelsky, N., Lee, S.H., Nguyen, J., Sanchez-Pernaute, R., Bankiewicz, K. *et al*. (2002) Dopamine neurons derived from embryonic stem cells function in an animal model of Parkinson's disease. *Nature*, **418**, 50–56.
52. Andersson, E., Tryggvason, U., Deng, Q., Friling, S., Alekseenko, Z., Robert, B., Perlmann, T. and Ericson, J. (2006) Identification of intrinsic determinants of midbrain dopamine neurons. *Cell*, **124**, 393–405.
53. Yamashita, H., Nakamura, T., Takahashi, T., Nagano, Y., Hiji, M., Hirabayashi, T., Amano, T., Yagi, T., Sakai, N., Kohriyama, T. *et al*. (2006) Embryonic stem cell-derived neuron models of Parkinson's disease exhibit delayed neuronal death. *J. Neurochem.*, **98**, 45–56.
54. Ye, W., Shimamura, K., Rubenstein, J.L., Hynes, M.A. and Rosenthal, A. (1998) FGF and Shh signals control dopaminergic and serotonergic cell fate in the anterior neural plate. *Cell*, **93**, 755–766.
55. Zhou, W., Schaack, J., Zawada, W.M. and Freed, C.R. (2002) Overexpression of human alpha-synuclein causes dopamine neuron death in primary human mesencephalic culture. *Brain Res.*, **926**, 42–50.
56. Baptista, M.J., O'Farrell, C., Daya, S., Ahmad, R., Miller, D.W., Hardy, J., Farrer, M.J. and Cookson, M.R. (2003) Co-ordinate transcriptional regulation of dopamine synthesis genes by alpha-synuclein in human neuroblastoma cell lines. *J. Neurochem.*, **85**, 957–968.
57. Wakayama, T., Tabar, V., Rodriguez, I., Perry, A.C., Studer, L. and Mombaerts, P. (2001) Differentiation of embryonic stem cell lines generated from adult somatic cells by nuclear transfer. *Science*, **292**, 740–743.
58. Regulier, E., Zala, D., Aebischer, P. and Deglon, N. (2004) Lentiviral-mediated gene transfer to model triplet repeat disorders. *Methods Mol. Biol.*, **277**, 199–213.
59. Lizee, G., Aerts, J.L., Gonzales, M.I., Chinnasamy, N., Morgan, R.A. and Topalian, S.L. (2003) Real-time quantitative reverse transcriptase-polymerase chain reaction as a method for determining lentiviral vector titers and measuring transgene expression. *Hum. Gene Ther.*, **14**, 497–507.